

Variation in the chemistry of the TiO₂-mediated degradation of hydroxy- and methoxybenzenes: electron transfer and HO[•]_{ads} initiated chemistry

Xiaojing Li, Jerry W. Cubbage, William S. Jenks*

Department of Chemistry, Iowa State University, 3760 Gilman Hall, Ames, IA 50011-3111, USA

Received 15 November 2000; received in revised form 3 May 2001; accepted 3 May 2001

Abstract

The early degradation product distributions from TiO₂-mediated photocatalytic degradations of a series of multiply hydroxylated benzenes and their methoxylated analogs is reported. The methoxylated compounds show a distinct trend away from ring-opening reactions that are attributed to electron transfer chemistry towards hydroxylations and demethylations that are attributed to hydroxyl-type chemistry. The initial rates of the reactions suggest that this is not simply due to the availability of the extra carbon sites. It is instead hypothesized that the compounds with hydroxyl groups are bound to the TiO₂ in such a way as to facilitate electron transfer and its subsequent chemistry. Addition of isopropyl alcohol to the degradations slows the degradations of the methoxylated compounds more than it does the hydroxylated compounds and particularly inhibits the demethylation and hydroxylation reactions. It is suggested that the question of whether an organic substrate must be bound to the photocatalyst at the time of excitation may be dependent on the type of chemistry being observed. © 2001 Elsevier Science B.V. All rights reserved.

Keywords: Photocatalysis; Titanium dioxide; Photodegradation; Langmuir–Hinshelwood model

1. Introduction

Photocatalytic oxidation of organic compounds by semiconductor oxides such as TiO₂ has attracted attention for treating contaminated water. Understanding of the chemical pathways of that degradation is of considerable practical interest due to the potential of incomplete mineralization, but is also a point of fundamental chemical interest. Although in early work, most of the oxidative chemical reactivity was attributed to surface bound hydroxyl radicals, in recent years, direct interaction between photogenerated holes and organics has gained recognition as an important process. Such single electron transfer reactions would seem to require direct adsorption of the organic to the semiconductor surface to be competitive with other reactions. This hypothesis allows one to test mechanistic proposals about the origin of certain transformations, on the assumption that hydroxyl-type chemistry might occur with a less rigorous binding requirement might be had, for instance, the Eley–Rideal (ER) formalism in which the binding event

can occur between the organic and the previously activated TiO₂.

In this paper, several methoxy- and hydroxy-substituted benzenes are chosen as model compounds, based on our previous studies on the degradation of aromatic compounds deriving from 4-chlorophenol degradation [1,2]. For these compounds, the early degradation steps are anticipated to be ring hydroxylation, demethylation, and ring-opening [3]. Consistent with work by other authors [4–6], we [1,2] have suggested that the ring-opening reactions are induced by single electron transfer, rather than hydroxyl-type chemistry.

Given the strong distance dependence of the rate of electron transfer and a presumption of a short lifetime for the valence band hole in hydrated TiO₂, it was hypothesized that subtle modification of the organic substrates in such a way as to lessen binding affinity might change the balance of hydroxyl-type and proposed electron transfer-type chemistry. Based on Lewis's binding studies [7,8], capping of phenolic groups to make methyl ethers was chosen. In this paper, we report the early degradation products of several hydroxy/methoxybenzenes, qualitative binding data, and a study on the effect of addition 2-propanol to the degradation mixture, a step that reduces the effective binding ability of some of the larger organic molecules.

* Corresponding author. Tel.: +1-515-294-4711; fax: +1-515-294-0105.
E-mail address: wsjenks@iastate.edu (W.S. Jenks).

2. Experimental section

2.1. Degradations, general

The water employed was purified by a Milli-Q UV plus system (Millipore) resulting in a resistivity more than $18 \text{ M}\Omega \text{ cm}^{-1}$. TiO_2 was Degussa P-25, which consists of 75% anatase and 25% rutile with a specific BET surface area of $50 \text{ m}^2 \text{ g}^{-1}$ and a primary size of 20 nm [9]. A 100 ml solution containing the desired concentration of starting material was prepared in water or buffer, and 50 mg of suspended TiO_2 was added into a cylindrical Pyrex vessel. The mixture was dispersed in ultrasonic bath for 5 min to disperse larger aggregates and then purged with O_2 and stirred for 15 min in dark before the irradiation was started. The mixture was continuously purged with O_2 throughout the irradiation. Irradiations were carried out in a mini Rayonet photochemical reactor with $8 \text{ W} \times 4 \text{ W}$ 360 nm “black light” lamps. Magnetic stirring and a fan insured maintenance of ambient temperature and adequate mixing. Samples (0.5 ml) were withdrawn from the reaction vessel at regular time intervals during the irradiation. They were centrifuged with an Eppendorf Netheler Hinz 5415C and filtered using $0.2 \mu\text{m}$ Whatman cellulose nitrate filter before HPLC analysis. For some reactions as noted, a Pyrex bottle with an outer water jacket through which water thermostatted at $30 \pm 0.5^\circ\text{C}$ was pumped continuously, was used.

Certain experiments were carried out with direct irradiation in the absence of TiO_2 . For these degradations, broadly irradiating 300 nm bulbs were used in the Rayonet. Other conditions were identical. In experiments where it indicated, 1 ml 30% H_2O_2 was added immediately before photolysis.

2.2. Dark adsorption

Equilibrium extents of adsorption onto TiO_2 were evaluated after equilibration for fixed periods with vigorous magnetic stirring and pH held at 7.0 with 5 mM phosphate buffer. Suspensions were prepared from 20 ml aliquots of solution with 50 mg TiO_2 . After allowing the desired contact time, an aliquot was removed, centrifuged, and syringe filtered through Millipore filters to remove TiO_2 . The residual concentration of compounds was determined by UV–VIS spectroscopy using a Shimadzu UV-2101 spectrometer. Kinetic study showed that the extent of adsorption reached a constant value after no more than 4 h for all compounds. For the quantitative adsorption experiments, at least 15 h equilibration was allowed before measurement.

2.3. HPLC analyses for kinetics

The concentration of compounds **1–6** were measured by HPLC using a HP 1050 instrument equipped with a ODS Hypersil C_{18} reversed phase column ($5 \mu\text{l}$ injection loop, 200 mm long, 2.1 mm i.d., $5 \mu\text{m}$ particle diameter).

All substances were detected by a diode array UV detector, monitored at 220, 255 and 290 nm. The mobile phase employed for the analysis of **1** was a mixture of 20 parts methanol and 80 parts water also containing 0.2% acetic acid. A mixture of 10 parts methanol and 90 parts of water containing 0.2% acetic acid was used for the analysis of the rest of the compounds. The flow rate was 0.5 ml min^{-1} . The identification of the intermediates by HPLC was performed by comparing the retention times and the UV spectra of authentic compounds. Samples under standard conditions were held at pH 7.0 using a 5 mM sodium phosphate buffer. The samples done at pH 4.0 were also held with 5 mM phosphate, and those at 8.5 held with 10 mM phosphate. The pH of 2.0 was achieved with perchloric acid.

2.4. GC–MS analysis for degradation product identification

Many runs were designed to determine products. These were done using the same 100 ml solutions, but without buffer. The pH was maintained at 7.0 ± 0.5 by careful addition of NaOH solution. Further analysis steps were as previously described [1]. Briefly, after an appropriate period of degradation, the solutions were centrifuged, filtered, and concentrated to 2–3 ml. For GC–MS analysis, silylation of the hydroxyl groups (including carboxylic acids) was required. For any given degradation, three types of data were collected. First, a run was treated as described above and then silylated. A second run would be collected, and then reduced with NaBH_4 before silylation. A third run would be treated with NaBD_4 before silylation. The two latter experiments were used to “count ketones and aldehydes” and revealed some compounds that did not survive GC without reduction. Compounds were identified by comparison to authentic sample when possible, and others are more tentatively identified as outlined below by analysis of the mass spectra.

GC–MS was done through a 25 m capillary DB-5 column on a Varian GC, coupled to a Magnum ion trap (Finnigan MAT) mass spectrometer. The temperature-program began at 50°C for 4 min, followed by a ramp at $15^\circ\text{C min}^{-1}$ to 280°C . Routine analysis with the same type of column and temperature-program was also done with an FID detected HP-5890-II GC. When multiple similar retention times are listed under a single peak, this indicates that two peaks were observed, but that more than one stereoisomer is to be expected.

2.5. Identification of peaks with authentic samples

The following compounds were prepared by literature methods and used as authentic samples to identify the indicated peaks: 3-hydroxypropionic acid [10] (peak 8); the monomethyl esters [11] of maleic (peak 9) and fumaric (peak 11) acids; methoxymaleic acid [12] (peak 29) was prepared by hydrolysis of methoxymaleic anhydride [13];

1,2,4,5-benzenetetraol [14] (peak 54); 2,3,4-trihydroxyglutaric acid [15] (peak 55). The compounds corresponding to peaks 17, 20, 33, and 34 were prepared as previously reported [1]. Starting material 4-chlorocatechol [16] was prepared as reported. 4-Chloro-1,2-dimethoxybenzene was prepared from 4-chlorocatechol and iodomethane [17].

The following compounds were obtained commercially and their silylated derivatives were used as authentic samples: methyl glycolate (peak 1), ethylene glycol (peak 2), lactic acid (peak 4), glycolic acid (peak 6), oxalic acid (peak 7), methyl hydrogen succinate (peak 10), malonic acid (peak 12), glyoxylic acid (peak 15), maleic acid (peak 18), succinic acid (peak 19), fumaric acid (peak 21), tartronic acid (peak 23), malic acid (peak 28), 2-methoxy-1,4-hydroquinone (peak 36), 2,4-dihydroxy-1,4-benzoquinone (peak 38), tartaric acid (peak 40). Starting materials 1,2,4-trimethoxybenzene, 3,4-dimethoxyphenol, and 4-chloro-2-methoxyphenol were also obtained commercially.

2.6. Identification of peaks by mass spectrometry

The data discussed in these paragraphs are taken from Table 1. Peak 3 — methyl hydrogen oxalate: the molecular weight (CI) is 176. The peak at $m/z = 161$ corresponds to loss of CH_3 (M-15). The fragment at $m/z = 117$ indicates loss of CO_2TMS . The fragment at 59 confirms CO_2CH_3 .

2.6.1. Peak 5 — methyl hydrogen malonate

The molecular peak of the silylated compound ($m/z = 190$) was found by CI. This compound probably contains only one TMS group because the fragment at $m/z = 147$ ($\text{CH}_3)_2\text{Si}-\text{O}-\text{Si}(\text{CH}_3)_3$, which indicates the presence of more than one TMS-O group, was not observed. Losses of methyl and COOCH_3 can be attributed to the peaks at $m/z = 175$ and 131. This compound is not reduced by NaBH_4 , giving the malonate monoester.

2.6.2. Peak 13

This compound cannot be silylated, indicating the absence of alcohols or carboxylic acids. The fragment $m/z = 115$ indicates loss of COOCH_3 , which is consistent with the fragment $m/z = 59$. Given the starting material and the molecular weight of this peak, it is very likely dimethyl methoxymaleate.

2.6.3. Peak 14 — methyl-2,3-dihydroxypropionate

The compound contains at least two TMS groups due to the presence of fragment at $m/z = 147$. Peaks at $m/z = 103$ (CH_2OTMS) and 102 (CHOTMS) indicate primary and secondary alcohol fragments, respectively. The fragment at $m/z = 205$ corresponds loss of COOCH_3 , consistent with the fragment at $m/z = 59$.

2.6.4. Peak 16 — methyl hydrogen tartronate

This compound is not reduced by NaBH_4 . It contains two TMS groups and one COOCH_3 , as inferred from $\text{CI} = 278$

and the fragments at $m/z = 147$ and 59. The formula of this compound should be $\text{C}_4\text{H}_4\text{O}_5(\text{TMS})_2$. The fragment at $m/z = 219$ (M- COOCH_3) also confirms the presence of the methyl ester. In addition, the secondary alcohol group was suggested by the peak at $m/z = 102$.

2.6.5. Peak 24 — dimethoxyphenyl formate

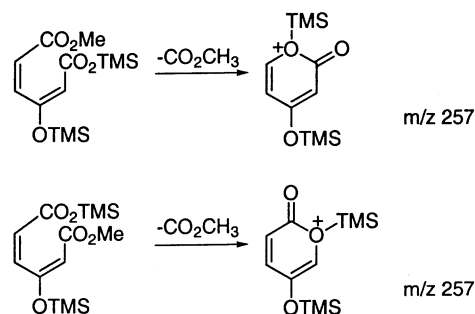
This compound cannot be silylated, indicating that there are no carboxyl or hydroxyl groups in the compound. The fragment at $m/z = 154$ could be attributed to dimethoxyphenol, whose loss of CH_3 will form the base peak $m/z = 139$. Given the starting material and the molecular weight of this peak, it is assigned to an isomer of dimethoxyphenyl formate. This is also consistent with our previous findings on the degradation of anisole [18].

2.6.6. Peak 25

This was only found in the degradation of **1**, and has a very similar MS pattern and retention time to peak 26. It is, therefore, presumed to be 2,4-, or 2,5-dimethoxyphenol.

2.6.7. Peak 30 — a monomethyl ester of 3-hydroxy muconic acid

This compound has high analogy to the ring opened compound from 1,2,4-benzenetriol [1]. The mass of the silylated compound is 316. It should have two TMS groups and one methyl ester based on the peak $m/z = 147$ and 59. The formula appears to be $\text{C}_7\text{H}_6\text{O}_5(\text{TMS})_2$, given the starting materials. The base peak $m/z = 257$ is correlated to loss of COOCH_3 (M-59). This peak and peak 48 appear to be the two different monomethyl esters of 3-hydroxy muconic acid. Given which is observed from which precursors, it appears likely that peak 30 is the 1-methyl ester.



2.6.8. Peak 31 and 32 — monomethyl ester of tartaric acid

This compound has three acids and/or alcohols and one methyl ester. It contains secondary alcohol ($m/z = 102$), and the fragments at $m/z = 219$ (M-161) and 161 are correlated to $\text{CH}(\text{OTMS})\text{COOTMS}$ and $\text{CH}(\text{OTMS})\text{COOCH}_3$, respectively. The mass (CI) of this compound is 380 which is the sum of above two fragments. Its precursor (in degradations of **6**) is reduced twice by NaBH_4 , and has a formula of $\text{C}_5\text{H}_8\text{O}_6(\text{TMS})_3$ which is a derivative of tartaric acid monomethyl ester.

Table 1
Intermediates observed in the partial photocatalytic degradations of **1–4** and **6**^a

Peak no.	Size from: 1–4 and 6	Intermediate	Reduced intermediate	Retention times	Formula weights	<i>m/z</i> values (relative abundance)
1	–, s, s, s, –			7.19	162	NaBH ₄ : 59 (20), 73 (25), 89 (70), 103 (30), 119 (50), 133 (8), 147 (100), 162 (2)
2	–, m, l, s, m			8.04	206	NaBH ₄ : 73 (33), 103 (15), 133 (8), 147 (100), 191 (25) NaBD ₄ : 73 (30), 103 (15), 104 (10), 133 (5), 147 (100), 191 (20), 193 (25)
3	–, l, l, s, m			8.13	176	59 (28), 73 (100), 89 (50), 117 (10), 161 (45)
4	–, s, s, s, s			9.06	234	NaBH ₄ : 73 (70), 117 (72), 133 (15), 147 (100), 191 (35), 219 (10) NaBD ₄ : 73 (65), 118 (90), 133 (10), 147 (100), 192 (45), 220 (20)
5	–, s, m, s, s			9.12	190	59 (22), 73 (40), 89 (100), 101 (15), 115 (10), 131 (16), 143 (8), 159 (6), 175(65), 190 (6)
6	–, l, l, s, m			9.19	220	NaBH ₄ : 73 (58), 103 (10), 133 (8), 147 (100), 161 (10), 177 (20), 205 (24), 220 (3) NaBD ₄ : 73 (55), 103 (10), 104 (8), 133 (10), 147 (100), 161 (10), 177 (15), 178 (10), 205 (15), 206 (12), 221 (5)
7	–, l, l, s, l			10.05	234	73 (84), 133 (5), 147 (100), 190 (18), 219 (12)
8	–, s, m, s, s			10.11	234	NaBH ₄ : 73 (25), 103 (10), 133 (10), 147 (100), 165 (8), 177 (25), 219 (35) NaBD ₄ : 73 (30), 104 (8), 133 (10), 147 (100), 165 (8), 178 (20), 220 (20)
9	–, m, m, s, –			10.29	202	59 (20), 73 (25), 89 (60), 113 (55), 126 (5), 143 (6), 157 (6), 171 (20), 187 (100), 202 (3)
10	–, –, –, s, –			10.35	204	59 (20), 73 (70), 75 (95), 89 (100), 105 (20), 115 (40), 129 (45), 173 (30), 189 (90), 204 (5)
11	–, m, s, m, –			10.47	202	59 (15), 73 (45), 89 (50), 113 (55), 126 (10), 143 (20), 159 (6), 171 (22), 187 (100)
12	–, m, m, m, ■			10.52	248	73 (29), 147 (100), 233 (16), 248 (6)

13	m, -, -, -, -		11.01	174	59 (35), 69 (100), 101 (25), 115 (95), 127 (20), 143 (70), 159 (45), 174 (10)
			11.30		
14	-, m, m, s, m		11.10	264	NaBH4: 59 (25), 73 (100), 89 (32), 102 (30), 103 (40), 117 (90), 131 (20), 147 (70), 163 (15), 189 (18), 205 (15), 234 (55), 249 (30) NaBD4: 59 (20), 73 (95), 89 (20), 103 (28), 104 (30), 119 (90), 135 (20), 137 (20), 147 (70), 163 (15), 190 (10), 191 (15), 207 (15), 235 (55), 251 (35)
15	-, -, -, -, s		11.21	308	73 (85), 103 (10), 117 (5), 131 (10), 133 (15), 147 (80), 177 (10), 191 (100), 219 (30), 221 (40), 265 (15), 293 (10)
16	-, m, m, s, l		11.48	278	59 (15), 73 (90), 89 (8), 102 (20), 130 (20), 131 (15), 133 (18), 147 (100), 163 (15), 219 (20), 235 (35), 263 (12)
17	-, -, s, s, -		11.51	260	NaBH4: 73 (50), 133 (10), 143 (25), 147 (100), 170 (25), 217 (10), 245 (30), 260 (10) NaBD4: 73 (55), 133 (10), 143 (15), 147 (100), 171 (20), 218 (5), 246 (20), 261 (10)
18	-, m, l, s, -		11.58	260	73 (35), 133 (7), 147 (100), 171 (20), 215 (5), 245 (22)
19	-, s, s, s, -		12.01	262	73 (30), 129 (8), 147 (100), 172 (8), 247 (28), 262 (3)
20	-, m, l, s, l		12.11	322	NaBH4: 73 (98), 101 (15), 102 (26), 103 (28), 117 (20), 133 (30), 147 (100), 189 (75), 205 (15), 217 (10), 292 (45), 307 (15) NaBD4: 73 (100), 102 (20), 103 (20), 104 (15), 105 (18), 117 (20), 133 (25), 147 (100), 190 (45), 191 (60), 207 (15), 292 (45), 239 (45), 309 (15)
21	-, s, m, s, -		12.26	260	73 (24), 143 (14), 147 (24), 245 (100)
22	-, m, s, s, m		12.34	292	NaBH4: 59 (30), 73 (100), 89 (15), 101 (20), 105 (15), 115 (10), 117 (60), 131 (10), 133 (35), 147 (80), 163 (15), 173 (18), 175 (15), 189 (12), 207 (10), 217 (10), 233 (10), 249 (14), 277 (8) NaBD4: 59 (20), 73 (80), 89 (15), 102 (15), 105 (10), 117 (10), 132 (20), 133 (35), 134 (35), 147 (100), 163 (20), 176 (20), 190 (12), 208 (10), 218 (10), 234 (15), 250 (40), 278 (20)
		or			
		or			
23	-, m, m, s, m		12.43	336	73 (89), 102 (32), 133 (28), 147 (100), 177 (4), 221 (16), 249 ((16), 292 (40), 293 (36), 321 (20)

Table 1 (Continued)

Peak no.	Size from: 1–4 and 6	Intermediate	Reduced intermediate	Retention times	Formula weights	<i>m/z</i> values (relative abundance)
24	m, –, –, –, –			13.01	182	53 (22), 55 (20), 69 (20), 75 (15), 89 (12), 93 (10), 111 (50), 125 (12), 139 (100), 154 (40), 182 (20)
25	l, –, –, –, –			13.20	226	73 (20), 153 (15), 181 (20), 196 (100), 211 (10), 226 (60)
				13.29		
26	l, –, –, –, –		i.e., 2	13.37	226	73 (85), 153 (10), 167 (10), 183 (15), 211 (90), 226 (100)
27	–, –, –, –, l			■3.43	350	NaBH ₄ : 73 (100), 101 (8), 133 (18), 147 (90), 175 (11), 189 (16), 217 (15), 233 (36), 245 (15), 307 (8), 333 (30), 335 (30) NaBD ₄ : 73 (100), 102 (12), 133 (18), 147 (80), 176 (10), 190 (16), 218 (10), 234 (36), 246 (10), 308 (8), 334 (20), 336 (20)
28	–, s, l, s, m,			■3.43	350	73 (100), 101 (8), 133 (18), 147 (90), 175 (11), 189 (16), 233 (36), 245 (24), 307 (8), 335 (12)
29	–, m, m, s, m			■3.46	290	73 (40), 147 (100), 201 (20), 217 (5), 245 (5), 275 (30), 290 (5)
30	–, s, l, s, –			■3.50	316	59 (12), 73 (52), 89 (14), 133 (12), 147 (18), 169 (22), 241 (6), 257 (100), 273 (8), 301 (12)
		and/or 				
31	–, –, –, –, m			■3.52	380	NaBH ₄ : 59 (10), 73 (100), 89 (15), 102 (18), 103 (32), 133 (32), 147 (52), 161 (20), 189 (18), 219 (28), 233 (15), 234 (20), 247 (55), 277 (10), 292 (10), 305 (18), 321 (10), 365 (16)
				■4.13		NaBD ₄ : 59 (10), 73 (100), 89 (10), 103 (15), 104 (20), 133 (32), 147 (65), 163 (15), 192 (5), 220 (28), 234 (30), 235 (25), 248 (55), 279 (10), 293 (10), 306 (18), 321 (10), 366 (16), 367 (14)

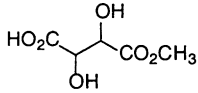
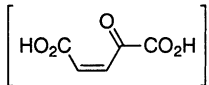
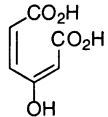
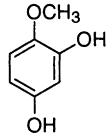
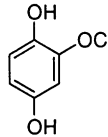
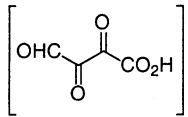
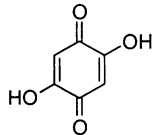
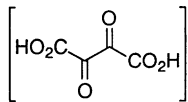
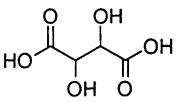
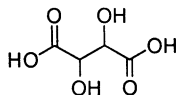
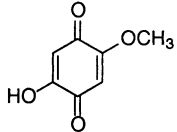
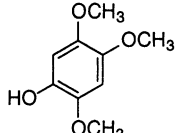
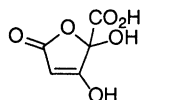
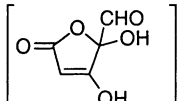
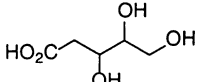
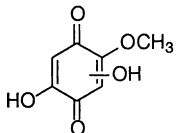
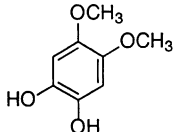
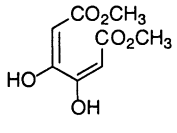
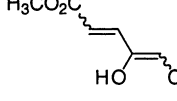
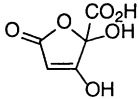
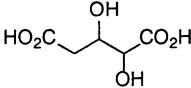
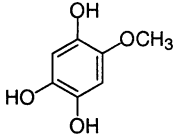
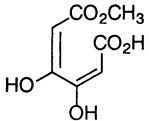
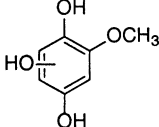
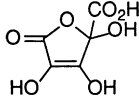
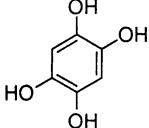
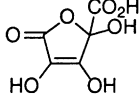
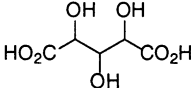
32	-, s, s, s, -		13.52	380	59 (10), 73 (100), 89 (15), 102 (18), 103 (32), 133 (32), 143 (15), 147 (52), 161 (20), 189 (18), 219 (28), 234 (64), 247 (55), 277 (10), 292 (10), 305 (18), 321 (10), 365 (16)	
33	-, -, m, -, -		14.13	■4.05	362	NaBH ₄ : 73 (100), 133 (12), 147 (38), 156 (18), 245 (8), 303 (8), 318 (20), 347 (12) NaBD ₄ : 73 (100), 133 (10), 147 (45), 157 (25), 246 (8), 304 (10), 319 (22), 348 (12)
34	-, -, s, -, -		■4.11	374	73 (16), 133 (16), 147 (24), 169 (8), 241 (4), 257 (100), 330 (8), 331 (16), 359 (14)	
35	-, s, -, -, -	 i.e., 3	■4.07	284	73 (40), 133 (12), 147 (10), 239 (10), 254 (100), 269 (15), 284 (50)	
36	-, m, -, -, -	 i.e., 4	■4.15	284	73 (80), 103 (20), 133 (12), 147 (10), 219 (10), 234 (25), 247 (36), 254 (100), 269 (15), 284 (50)	
37	-, s, -, -, m		■4.19	424	NaBH ₄ : 73 (100), 102 (15), 103 (20), 117 (25), 129 (15), 133 (20), 147 (70), 189 (10), 205 (15), 217 (30), 219 (25), 245 (10), 292 (50), 319 (10), 379 (3), 409 (8) NaBD ₄ : 73 (100), 103 (15), 104 (12), 117 (20), 130 (20), 133 (20), 147 (80), 190 (10), 207 (15), 219 (20), 221 (25), 248 (10), 293 (50), 321 (10), 382 (3), 412 (8)	
38	-, m, m, l, l		■4.28	284	73 (20), 113 (5), 147 (5), 194 (5), 224 (5), 254 (100), 269 (30)	
39	-, -, -, -, m		■4.32	438	NaBH ₄ : 73 (100), 102 (10), 133 (10), 147 (64), 189 (30), 219 (22), 277 (10), 292 (65), 305 (12), 333 (6), 367 (10), 423 (20)	
			■4.58		NaBD ₄ : 73 (100), 103 (10), 133 (10), 147 (64), 191 (30), 220 (22), 279 (10), 293 (65), 306 (12), 334 (6), 369 (10), 425 (20)	
40	-, s, s, s, -		■4.32	438	73 (100), 133 (20), 147 (64), 189 (12), 219 (22), 292 (74), 305 (12), 333 (6), 423 (8)	

Table 1 (Continued)

Peak no.	Size from: 1–4 and 6	Intermediate	Reduced intermediate	Retention times	Formula weights	<i>m/z</i> values (relative abundance)
				14.58		
41	–, –, s, m, l			14.42	226	73 (30), 113 (15), 137 (12), 155 (12), 168 (10), 183 (60), 211 (100), 226 (10)
42	s, –, –, –, –			14.48	256	73 (60), 89 (10), 183 (20), 199 (25), 211 (25), 226 (55), 241 (40), 256 (100)
43	–, s, –, s, l			14.54	376	73 (80), 99 (10), 133 (12), 147 (55), 163 (25), 171 (20), 215 (10), 221 (10), 231 (10), 259 (100), 273 (5), 287 (10), 303 (10), 332 (10), 333 (15), 361 (20), 376 (3)
44	–, –, –, s, s			■.04	438	NaBH ₄ : 73 (100), 102 (10), 103 (15), 117 (15), 129 (15), 133 (20), 147 (70), 189 (15), 205 (10), 217 (50), 231 (20), 245 (95), 275 (8), 292 (8), 305 (5), 333 (15), 348 (5), 423 (10)
				■.12		NaBD ₄ : 73 (100), 103 (10), 104 (10), 117 (15), 130 (15), 133 (15), 147 (50), 189 (15), 207 (10), 218 (50), 234 (10), 247 (80), 276 (8), 292 (8), 307 (5), 336 (15), 350 (10), 426 (10)
45	–, s, s, s, m			■.11	314	73 (35), 113 (10), 127 (10), 147 (10), 254 (30), 269 (10), 284 (100), 299 (12), 314 (65)
46	–, m, –, –, –			■.15	314	73 (65), 147 (10), 183 (20), 211 (16), 254 (22), 272 (25), 284 (45), 299 (50), 314 (100)
47	–, m, –, –, –			■.22	346	59 (10), 73 (20), 89 (10), 147 (5), 156 (15), 171 (5), 199 (15), 257 (8), 259 (8), 271 (12), 287 (100), 303 (8), 331 (20), 346 (3)
				■.40		
48	–, s, –, l, –			■.28	316	59 (5), 73 (15), 95 (5), 123 (10), 147 (12), 167 (5), 169 (5), 227 (5), 241 (5), 257 (100), 285 (5), 301 (30), 316 (5)
				■.40		

49	–, s, m, m, l	 i.e., peak 43		15.33	452	NaBH ₄ : 73 (100), 101 (8), 102 (8), 129 (12), 131 (10), 133 (16), 147 (65), 217 (30), 245 (60), 291 (10), 319 (25), 377 (20), 437 (20)
				15.38		NaBD ₄ : 73 (100), 102 (10), 103 (8), 131 (15), 133 (16), 147 (65), 219 (20), 247 (70), 293 (35), 321 (20), 379 (10), 439 (20)
50	–, l, m, l, –	 i.e., 6		15.35	372	73 (5), 123 (5), 157 (10), 169 (15), 201 (10), 254 (10), 342 (40), 372 (100)
51	–, l, m, m, s			15.43	404	59 (5), 73 (18), 109 (5), 147 (10), 156 (10), 199 (5), 257 (5), 259 (4), 271 (10), 287 (100), 315 (5), 345 (10), 361 (20), 389 (20)
52	–, s, l, –, –			15.45	372	73 (80), 147 (8), 269 (50), 284 (12), 299 (12), 342 (75), 357 (20), 372 (100)
53	–, s, –, –, s			15.54	464	73 (75), 133 (15), 147 (50), 221 (10), 259 (10), 319 (10), 333 (5), 347 (100), 393 (5), 421 (20), 449 (25)
54	–, s, s, s, s			16.00	430	73 (45), 147 (15), 179 (8), 207 (8), 254 (5), 342 (10), 415 (5), 430 (100)
55	–, s, –, m, l	 i.e., peak 53		16.22	540	NaBH ₄ : 73 (100), 102 (15), 133 (15), 147 (45), 189 (25), 277 (20), 292 (80), 293 (20), 333 (20), 361 (10), 407 (35), 435 (10), 525 (15)
				16.29		NaBD ₄ : 73 (100), 103 (10), 133 (15), 147 (45), 191 (25), 279 (20), 293 (80), 294 (20), 335 (10), 363 (10), 409 (30), 437 (10), 527 (15)

^a Initial conditions: concentration of starting material = 0.001 g/l, volume = 100 µl, [NaBH₄] = 0.5 g l⁻¹, t = 30, 90, 30, 30, and 60 min for 1–4 and 6, respectively. Gas chromatography was obtained with the following temperature-program and a 200-m column: initially at 50°C, hold time = 4 min; ramp from 50 to 280°C at 15°C min⁻¹; at 280°C, hold time = 5 min. Peak sizes are qualitative representations (small, medium, large) of the magnitude of the peaks. Repetitions were carried out to times that maximized the number of intermediates, but control experiments showed that the relative qualitative magnitudes of the early degradation products were largely unaffected. Retention times given in minutes. Formula weights are taken from CI-MS runs. “intermediates” shown in brackets were only observed as the reduced product shown in the same run.

2.6.9. Peak 37 — 2,3,4-trihydroxybutanoic acid

The mass of silylated compound is 424. Fragments at $m/z = 103$ and 102 indicate primary and secondary alcohol fragments, respectively. The presence of $\text{CH}(\text{OTMS})\text{CH}_2(\text{OTMS})$ is consistent with the peak at $m/z = 205$. Peak $m/z = 117$ corresponds to COOTMS , and 219 implies the group $\text{CH}(\text{OTMS})\text{COOTMS}$. The molecular weight 424 is the sum of 205 and 219 . Furthermore, its precursor is reduced three times by NaBH_4 .

2.6.10. Peak 42 — 2,4,5-trimethoxyphenol

It is only found in the photodegradation of **1**. Due to lack of the fragment $m/z = 147$, this compound contains only one TMS group. It is not reduced by NaBH_4 . The starting material and apparent formula of $\text{C}_9\text{H}_{12}\text{O}_4(\text{TMS})$ give rise to the proposed structure.

2.6.11. Peak 44

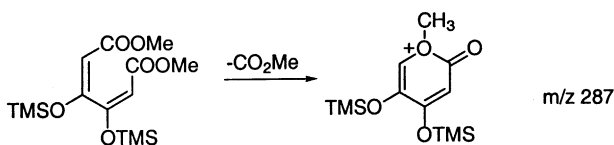
The mass of the silylated compound is 438 (from CI). Fragments at $m/z = 103$, 102 and 205 correspond to $\text{CH}(\text{OTMS})\text{COOTMS}$. The presence of COOTMS was confirmed from the peak at $m/z = 117$. The fragment at $m/z = 217$ may be obtained by losing 90 (TMSOH) from the group $[\text{CH}(\text{OTMS})\text{CH}(\text{OTMS})\text{CH}_2(\text{OTMS})]$ which $m/z = 307$. The remaining group is CH_2 ($438 - 117 - 307 = 14$). Thus, it is suggested that the compound is 2,3,4-trihydroxypentanoic acid.

2.6.12. Peak 45

This compound is not specifically identified. Given the peak at $m/z = 147$ and the mass, it should have two TMS groups. Given an apparent formula of $\text{C}_7\text{H}_6\text{O}_5(\text{TMS})_2$, we suggest the peak is a dihydroxymethoxybenzoquinone. As previously discussed [1,2], benzenetriol and benzenetetraol oxidize to the corresponding quinones on handling, thus, the quinones are observed whether or not they are part of the original mixture.

2.6.13. Peak 47 — dimethyl *cis,cis*-3,4-dihydroxybutanoate

The mass of the silylated compound is 346 from CI. It is only observed in the photodegradation of 4,5-dimethoxybenzene-1,2-diol (peak 46). It has at least two TMS groups and one methyl ester based on the peaks at $m/z = 147$ and 59 . Given the starting material, it should not have more than eight carbons. Thus, the formula is $\text{C}_8\text{H}_8\text{O}_6(\text{TMS})_2$. The base peak $m/z = 287$ is correlated to loss one COOCH_3 ($M-59$). The compound is thus, assigned as dimethyl *cis,cis*-3,4-dihydroxybutanoate.



2.6.14. Peak 48 — a monomethyl ester of 3-hydroxymuconic acid

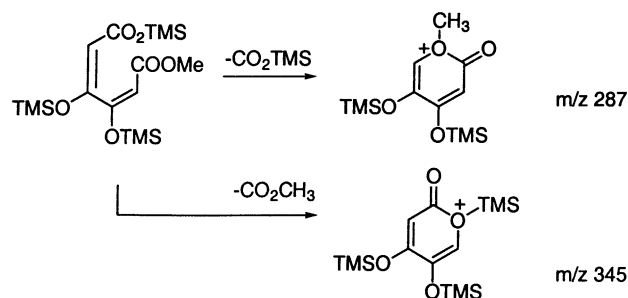
The mass spectrum of this compound is nearly same as the spectrum of peak 30, but the GC retention time is about $1\text{ min } 40\text{ s}$ longer than that of the peak 30. It was observed as a large peak in the photodegradation of 4-methoxyresorcinol and not found in the photodegradation of 2-methoxyhydroquinone. The formula of this compound is $\text{C}_7\text{H}_6\text{O}_5(\text{TMS})_2$. It is suggested that this is the 6-methyl 3-hydroxymuconate. See the explanation of peak 30.

2.6.15. Peaks 43 and 49

Peak 43 is observed only when reduction is not done to the sample. Peak 49 is only observed when reduction is carried out, and has a mass two units greater than peak 43. Peak 49 has been reduced twice, as confirmed by the NaBD_4 experiment. It also appears as two closely running peaks on the GC, consistent with two dialcoholic diastereomers. It has a mass spectral pattern similar to that of the TMS derivatives of the 2,4-dihydroxyglutaric acids [1], but has a different retention time. Combining these observations, it is suggested that peak 49 is the TMS derivative of 2,3-dihydroxyglutaric acid. The assignment of peak 43 as a tautomer of 2,3-dioxoglutaric acid is based on the assignment of peak 49. The molecular weight of 376 indicates three TMS groups, consistent with the $m/z = 147$ fragment. It is definitely reduced (apparently to peak 49) by borohydride, thus yielding the only sensible formula of $\text{C}_5\text{HO}_5(\text{TMS})_3$. The base peak of 259 indicates of loss of CO_2TMS . All of these factors are consistent with the stated assignment.

2.6.16. Peak 51 — methyl hydrogen 3,4-dihydroxybutanoate

The mass of the silylated compound is 404 . Given that mass, and the peaks at $m/z = 147$ and 59 , it has three TMS groups and at least one methyl ester. It should have no more than seven carbons, given the starting materials. Like peak 47, it has a base peak at $m/z = 287$. This represents loss of CO_2TMS from peak 51. The most reasonable formula is $\text{C}_7\text{H}_5\text{O}_6(\text{TMS})_3$. Loss of CO_2CH_3 is indicated by the peak at $m/z = 345$. These data indicate the monoester of 3,4-dihydroxybutanoic ester is the likely structure.



2.6.17. Peak 52

This compound is not uniquely identified. The mass indicates three TMS groups. Given the mass and comparatively

minor fragmentation, the compound is likely to be a fairly simple aromatic, with $C_7H_5O_4(TMS)_3$ as the most likely formula. The structure we suggest is an isomer of methoxybenzenetriol, e.g. a hydroxylation product of **3**.

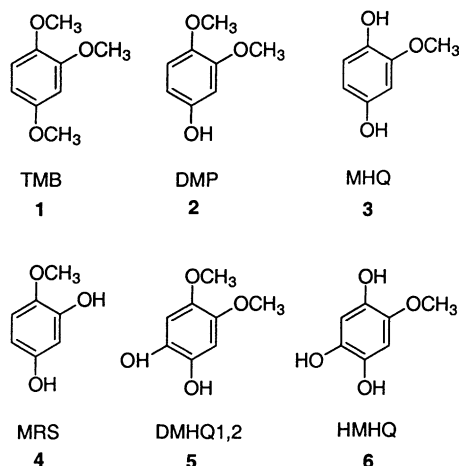
2.6.18. Peak 53 — 5-oxo-2,3,4-trihydroxy-2,5-dihydrofurancarboxylic acid

This compound does not survive the reduction treatment. As with peaks 43 and 49 above, it appears to be the precursor to peak 55, which was verified by comparison to authentic material.

3. Results

3.1. Degradation products of hydroxymethoxybenzenes

The initial set compounds used as starting materials for degradations are shown in Scheme 1. The choices were driven by two concerns. Compounds **1–4** are all close derivatives of 1,2,4-benzenetriol, which had previously been shown to undergo mainly a ring cleavage reaction that we had hypothesized derived from electron transfer from the substrate to the TiO_2 . The methyl groups were expected to interfere with the specific binding mode to TiO_2 in which *ortho*-oxygen bind to the titanium [8]. These four compounds have varying degrees of methylation, which should interfere with this tight binding. Compounds **5** and **6** are similar, but have a fourth oxygenation and are early degradation products of some of the other compounds. The essential hypotheses to be tested are that (a) good binding leads to rapid electron transfer, and thus, ring-opening reactions, and (b) that ease of oxidation also leads to ring-opening reactions at the expense of HO^\bullet -type chemistry. Finally, the main interest was in examining the primary and near-primary degradation products. The complete set of observed products is given below, but we present no further discussion on the comparatively small partial degradation products.



Scheme 1.

Degradations were carried out in separate experiments designed for HPLC detection and for GC detection. The standard conditions for the HPLC-detected runs were 100 ml aqueous samples, with 2 mM of the starting material dissolved and 50 mg of TiO_2 (Degussa P25) in suspension. The pH was controlled by a phosphate buffer (5 mM) to 7.0, and the solutions were saturated with O_2 . Small samples were periodically removed, filtered to remove the TiO_2 particles, and directly analyzed. In general, although several products could be identified in any given degradation, many polar products would overlap with short retention times and many minor products were not detected at all. As a result, HPLC-detected experiments were used mainly for qualitative “first runs” and for kinetics experiments described below.

The use of GC alleviated the overlap problem and allowed identification of a great deal more intermediates. In general, several degradations were carried out, each with slightly different conversion of the starting material in order to insure observation of the primary degradation products. For GC detection, the buffer was not used and the pH was kept within 0.5 units of 7.0 by careful titration with NaOH solution during photolysis. Samples were analyzed after a single period of time. The analysis, as previously described [1], involved removal of the solvent and functionalizing all exposed hydroxyl groups with TMS before GC analysis. Runs were repeated and treated with $NaBH_4$ or $NaBD_4$ before silylation.

The products obtained from the degradations are listed in Table 1, where every unique GC peak has a number, regardless of which degradations it was observed from. In the table, formula weights obtained from CI-MS are listed in one column and EI-MS fragmentations are listed in another. If a peak was observed with only silylation (i.e. without reduction), it is listed under the column “intermediate”. If it is observed only in the runs that were treated with $NaBH_4$ or $NaBD_4$, it is listed under the column headed “reduced intermediate”. In the latter case, one or more precursors is listed in the “intermediate” column, as deduced from the structure of the reduced intermediate and the deuterium count. If that precursor was not observed in the non-reduced runs, it is listed in brackets. The “size” column gives a qualitative rating of the size of the GC peak for each of the given starting materials. The maximum number of intermediates was observed with runs to about 50% conversion of starting material.

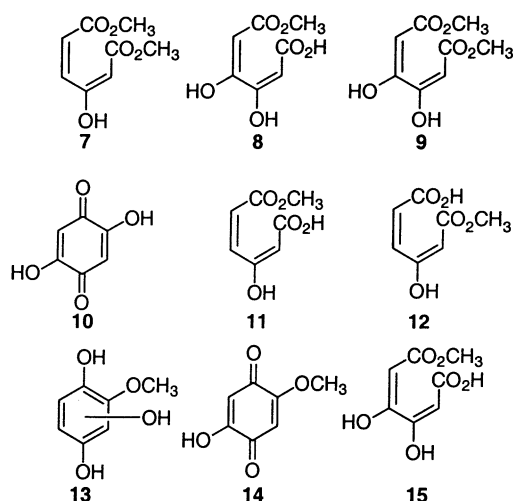
About two-thirds of the compounds identified in Table 1 were verified with authentic samples. The remainder are identified from the mass spectra and precedent among these and other previously investigated compounds. Details are found in Section 2. Finally, it must be mentioned that only a single tautomer is drawn for each of these compounds. In most cases, the illustrated tautomer is one chosen to show the obvious relationship between the starting material and the degradation product.

Unless otherwise stated, degradations were carried out under one of these sets of standard conditions. Also, unless

otherwise stated, control experiments showed that all three major components — 360 nm light, TiO₂, and O₂ — were required for significant degradation to occur on the time scale of the measurements.

3.1.1. 1,2,4-Trimethoxybenzene (**1**)

Only a modest number of intermediate degradation products are observed. The largest peaks (25 and 26) are observed for the dimethoxyphenol demethylation products. A moderate sized peak 24 is observed that corresponds to a dimethoxyphenyl formate. A small peak 42 is observed that corresponds to a hydroxylation product. All of these products are attributed to hydroxyl-type chemistry. Ring-opened products with five- or six-contiguous carbons are notably absent. Among the peaks corresponding to smaller compounds, peak 13, corresponding to dimethyl methoxymaleate, is most prominent. Furthermore, since six carbon ring-opened products were easily observed in other cases, the non-observation of dimethyl-3-methoxymuconate is taken to imply that it is formed in only trace amounts or not at all, rather than that it is degraded so quickly as to not be observable.



3.1.2. 3,4-Dimethoxyphenol (**2**)

A considerably greater number of intermediate degradation products were observed from **2** than **1**. Nonetheless, it appears that almost all the primary chemistry is of the hydroxyl radical-type (see also data in Section 3.2) The expected major direct ring-opening product, dimethyl-3-hydroxymuconate (**7**) was not observed. Instead, the two largest peaks corresponded to hydroxylation and demethylation (**6**, peak 50) and ring-opening accompanied by hydrolysis and hydroxylation (**8**, peak 51). It is not possible to determine the order of the three reactions that must occur for **8** to be formed; the absence of **7** indicates that it is unlikely that ring-opening is the first reaction of the sequence. Of the medium-sized peaks, **5** (peak 46) and **3** (peak 36) appear to be primary products due to hydroxylation and demethylation, respectively. Ring-opened compound **9** (peak 47) appears to be derived from **5**.

2,5-Dihydroxybenzoquinone (**10**) (peak 38) may actually represent the corresponding benzenetetraol that has been dark-oxidized by the presence of O₂, since most quinones are reduced under photocatalytic conditions [32]. The small peak 48 (**11**) represents a ring opened compound with six contiguous carbons, but it quite clearly is not a primary product due to the loss of the methyl group.

3.1.3. 2-Methoxyhydroquinone (**3**)

Because it is a hydroquinone, **3** oxidizes to the corresponding methoxybenzoquinone in the dark as long as O₂ is present. However, control experiments showed that the concentration of the benzoquinone declines rapidly when light is applied to the system (i.e. under “normal” conditions). It is also found that **3** decomposes beyond the corresponding benzoquinone under dark conditions. However, the dark products do not correspond to those that are observed under photocatalytic conditions. By GC, the major dark degradation product had a retention time of 20.23 min and a molecular weight above 600. This was present only in trace quantities with the photocatalytic runs.

One of the two large peaks corresponds to the direct ring-opening product **12** (peak 30, see Section 2). Peak 52 represents a hydroxylation product that we take to have the form of **15**. The mid-sized peaks show hydroxylation (peak 50), hydroxylation and opening (**8**, peak 51), and hydroxylation and demethylation in addition to dark oxidation (**10**, peak 38). It would, thus, appear that hydroxylation is the major primary step, but that it is accompanied by significant ring-opening.

3.1.4. 4-Methoxyresorcinol (**4**)

Because it is not a hydroquinone, **4** is considerably more stable than **3** in the presence of O₂. No dark degradation was observed; direct irradiation in the absence of TiO₂ led to its decomposition about 10 times slower than that under normal conditions. Again, the products were different and the direct irradiation products were not significant under normal conditions.

Both hydroxylation (**6**, peak 50) and ring-opening (**11**, peak 48) products appear as major primary degradation products. The other large peak (**10**, peak 38) is clearly a secondary product derived from hydroxylation and demethylation. The quinone derived from a simple hydroxylation (**14**, peak 41) and the product derived from both hydroxylation and ring-opening (**15**, peak 51) are observed as mid-sized peaks. Clearly ring-opening and hydroxylation are competitive processes for this compound.

In a separate experiment, degradation of **4** was carried out by 300 nm photolysis of solutions without TiO₂, but containing H₂O₂ as a source of hydroxyl radicals. The major degradation product was **6**, consistent with the supposition that arene hydroxylation is chemistry of the hydroxyl radical. Some ring-opened products with only a few carbons were observed, but **11** appeared only as a tiny trace peak.

3.1.5. 3,4-Dimethoxy-*o*-hydroquinone (**5**)

Compound **5** was chosen as one of the reasonably accessible early degradation intermediates that also fit in with the rest of the starting materials. Unfortunately, control experiments showed that **5** was too unstable under otherwise “normal” dark conditions to do proper degradations. It immediately oxidized to the corresponding benzoquinone and degraded further into other mainly unidentified products. The identifiable product formed in the greatest preponderance was **9**.

3.1.6. 4-Hydroxy-2-methoxyhydroquinone (**6**)

In dark, otherwise standard, conditions, **6** oxidizes to the corresponding benzoquinone (**14**). In contrast to the above example, however, the benzoquinone is stable under those conditions for a period of hours. As a result, TiO₂-mediated photocatalytic degradations of **6/14** were carried out. The quinone is quickly decomposed, and no further cyclic compounds were observed, save for the demethylated **10**. Although, the direct ring-opening intermediate **8** (peak 51) is only a minor peak, the five-contiguous-carbon peaks 49 and 55 are very large.

3.2. Degradation kinetics

Degradation kinetics were measured at pH 7.0 by periodic withdrawal of small samples, removal of the TiO₂, and analysis of the remaining starting material by HPLC. In general, it was observed that degradations went with first-order decays for at least 2–3 half-lives of the material. The rate constants obtained by fitting the concentration versus time plots are of course dependent on sample geometry, illumination intensity, and so on, but were internally reproducible to approximately 10% variation.

Degradations were carried out at pH 8.5, 7.0, 4.0, and 2.0 for 3,4-dimethoxyphenol (**2**). Observed rate constants were $(12.9 \pm 0.5) \times 10^{-3}$, $(19.6 \pm 0.8) \times 10^{-3}$, $(9.0 \pm 0.8) \times 10^{-3}$, and $(7.5 \pm 0.2) \times 10^{-3} \text{ min}^{-1}$, respectively, where the error limits are standard deviations of the fits. The rest of the degradations were carried out at pH 7.0. Compounds **3**, **4**, and **5** would appear to be obvious degradation products of **2** by demethylation or hydroxylation, yet each of them is a small peak. The reason for this is clarified by the rate constants obtained at pH 7 for each of their degradations. They degrade at $(33.4 \pm 0.8) \times 10^{-3}$, $(39.5 \pm 0.2) \times 10^{-3}$, and $(85 \pm 1) \times 10^{-3} \text{ s}^{-1}$, respectively. Thus, it is likely that they are small peaks simply because they are degraded faster than they are created. A modest decay rate constant for **1** of $(16.7 \pm 0.8) \times 10^{-3} \text{ s}^{-1}$ is also probably responsible for the very modest quantity of observed primary decomposition products.

The initial rates of photocatalytic degradations often show a dependence that can be successfully modeled with the Langmuir–Hinshelwood (LH) form

$$r_0 = \frac{k_{\text{LH}} K C_0}{1 + K C_0} \quad (1)$$

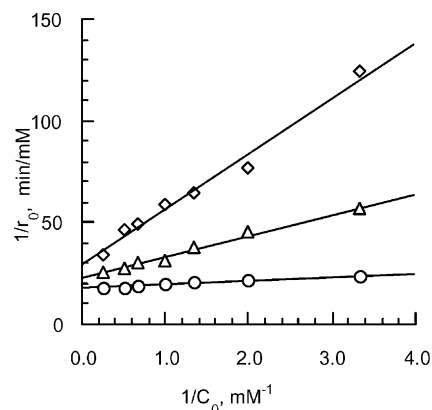


Fig. 1. Langmuir–Hinshelwood plot of the degradation rates of **1** (diamonds), **2** (triangles), and **4** (circles). Data were obtained at $30 \pm 0.5^\circ\text{C}$. Aside from temperature and concentration, other standard conditions were used.

where k_{LH} is an effective rate constant and K the classically taken as a binding constant between the organic adsorbate and the TiO₂ particles. The initial rates and concentrations are given by r_0 and C_0 . The equation can be linearized to the form

$$\frac{1}{r_0} = \frac{1}{k_{\text{LH}}} + \frac{1}{k_{\text{LH}} K} \frac{1}{C_0} \quad (2)$$

Decomposition data were acquired in a jacketed cell at $30.0 \pm 5^\circ\text{C}$ for compounds **1**, **2**, and **4** over a range of concentrations from 0.3 to 4.0 mM. The values of k_{LH} and K obtained from the plots, shown in Fig. 1, are given in Table 2. Compound **3** was excluded from the group due to difficulties in measuring its total concentration due to its nature as an easily air-oxidizable hydroquinone.

3.3. Dark adsorption and the effect of isopropyl alcohol

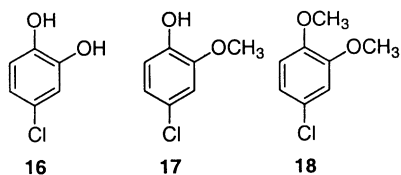
It is well understood that the LH form is simply an example of saturation kinetics and that a number of different mechanistic explanations can give rise to the same general appearance, including degradation mechanisms that do not include binding of the substrate to the TiO₂ [19–21]. Direct binding studies were thus desirable to correlate to the kinetic and product study data. In particular, it was of interest to look at of hydroxy/methoxy derivatives that included an *ortho*-dihydroxy system because of the bidentate binding model proposed by Lewis et al. [8]. However, this *ortho*-hydroquinone structure activates the molecules for air

Table 2
Langmuir–Hinshelwood fits of degradations of **1**, **2** and **4**^a

Compound	k_{LH} ($\mu\text{M min}^{-1}$)	K (mM^{-1})
1	34 ± 3	1.1 ± 0.2
2	45 ± 2	2.2 ± 0.2
4	56 ± 1	9.0 ± 0.9

^a Uncertainties are from standard deviations of the fit.

oxidation, making the measurements difficult and ambiguous. As a result, the deactivated 4-chloro series illustrated below was used for kinetic measurements, and binding isotherms were obtained for **16** and **18**.



Samples of known initial substrate concentration were prepared with identical suspensions of TiO_2 , buffered to pH 7.0. After a period of time long enough to insure equilibrium adsorption, they were filtered to remove the TiO_2 and the organic bound to it before determining the substrate concentration in the filtrate by UV. The isotherms were obtained from 20 ml mixtures containing 50 mg of TiO_2 . To additionally probe the binding, the experiments were repeated with 1% isopropyl alcohol (131 mM) added. The expectation was that the more weakly binding system might be displaced from the TiO_2 by the alcohol more than the more strongly binding counterpart. Confirmation of that expectation is seen by inspection Fig. 2, in which the bound quantity of the organic (expressed as the adsorbed concentration per gram TiO_2) is plotted against the equilibrium solute concentration both with and without *i*-PrOH.

Rates of degradation were obtained for compounds **1**, **2**, **4**, and **16–18** under the standard conditions and with 1% *i*-PrOH added. These data are shown in Table 3. The striking feature is that the compounds is the relationship between the number of blocked (i.e. methylated) OH positions and the ratio of k to $k_{i\text{-PrOH}}$. The last row of the table shows that the greater the degree of methylation, the more the degradation was slowed by alcohol addition.

The effect of isopropyl alcohol on the products was also briefly examined. In general, hydroxylation and demethylation products were suppressed relative to ring-opening. For compound **2**, degradation of all intermediates was made faster — relative to degradation of the starting material — as evidenced by the comparative paucity of partially degraded material at similar conversions of **2** with *i*-PrOH as compared to the original runs.

For compound **4**, whose original degradations showed a mixture of several hydroxylation/demethylation products along with ring-opened materials, suppression of

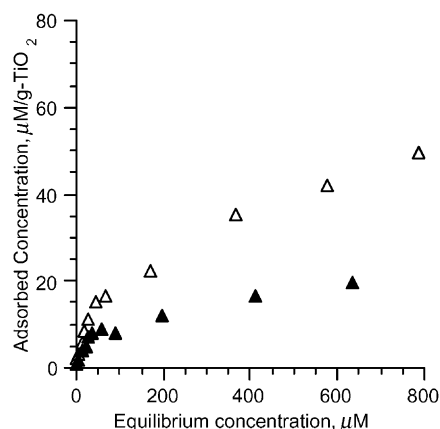
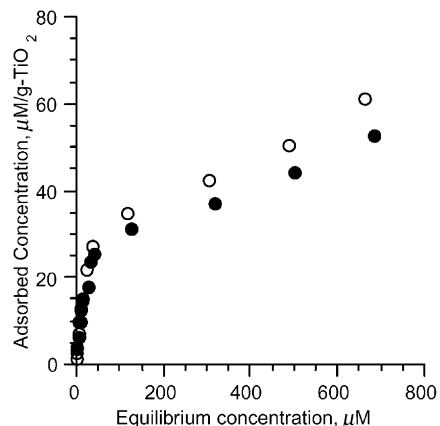


Fig. 2. Adsorption isotherms for 4-chlorocatechol **16** (circles) and 4-chloroveratrole **18** (triangles). Shown are isotherms obtained both without (open symbols) and with (filled symbols) 1% added isopropyl alcohol.

the hydroxylation products by *i*-PrOH was particularly straightforward to diagnose. Of the three major hydroxylation/demethylation products in the original runs (**6**, **10**, and **14**), only **14** remained as anything but a minor peak. Ring-opened products, particularly **11**, appeared relatively unaffected by the addition of the alcohol.

The initial rates of decay of **16–18** were also studied as a function of initial concentration. As can be seen in Fig. 3, only the initial rates of decay of **16** are described by Eq. (1) under our conditions. The decay time constants cited in Table 3 correspond well to the rates observed at 2 mM in

Table 3
Decay time constants with and without *i*-PrOH^a

Compound	Decay time constant (10^{-3} min^{-1})					
	1	2	4	16	17	18
k (standard conditions)	16.7	18.6	39.5	6.6	11.0	15.1
$k_{i\text{-PrOH}}$ (1% <i>i</i> -PrOH added)	2.0	6.6	30.6	2.3	1.9	1.0
$k/k_{i\text{-PrOH}}$	8.4	2.2	1.3	2.9	5.8	15.1

^a Standard conditions used, i.e. pH 7.0, 2 mM starting concentration.

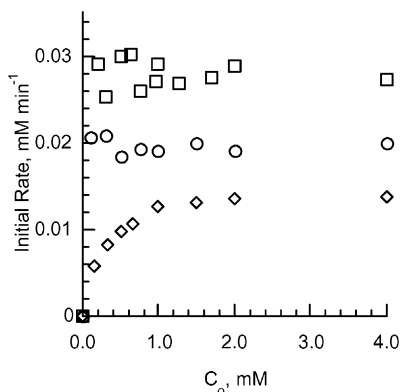


Fig. 3. Initial rates of decomposition of compounds **16** (diamonds), **17** (circles), and **18** (squares).

the figure. Parameters k_{LH} and K of $15 \pm 1 \mu\text{M min}^{-1}$ and $4.0 \pm 0.2 \text{ mM}^{-1}$, respectively, were obtained.

4. Discussion

The product study of the photocatalytic degradation of these compounds joins those of hydroquinone [1] 4-chlorocatechol [2] anisole [18] and various dimethoxybenzenes [3] in presenting a picture that fairly convincingly shows that there is a fundamental difference in the chemistry that leads to hydroxylation of arenes or loss of their alkyl groups and the chemistry that leads to their ring-opening. Both addition of HO or CH₃O substituents and the presence of HO over CH₃O favor ring-opening over the other reactions. In the series of compounds **1–4**, there is a clear trend in the primary degradation chemistry away from the hydroxylation and toward ring-opening, which is culminated in the previously reported degradation of 1,2,4-benzenetriol [1], where ring-opening is the near exclusive process. We suggest that this trend is due to the better binding of the hydroxylated substrates to the TiO₂, which specifically facilitates electron transfer, and thus, the ring-opening. The differential response to methoxylation also suggests that the possibility that electron transfer from the organic substrate to the surface bound hydroxyl radical [1] is unlikely.

The details of the mechanism of the ring-opening reaction remain somewhat speculative. After electron transfer, the hydroxylated/methoxylated benzene is, in effect, a semiquinone. In non-aqueous systems, Fox and others showed that electron transfer from olefins to TiO₂ was the first step in a mechanism that leads to oxidative cleavage that apparently proceeds through a dioxetane, but were never able to determine directly whether the nascent radical cation reacted with neutral O₂ or superoxide [22–25]. Though O₂ is surely more abundant, Pichat has carried out experiments using superoxide dismutase in related ring-opening reactions that seem to strongly implicate superoxide as a reactant [4,5,26]. Furthermore, Foote showed that the

interaction with superoxide with substituted catechols in acetonitrile could also lead to the same kinds of cleavage reactions observed here, also presumably via the semiquinone [27]. It has thus been suggested that superoxide reacts with the initially formed radical, [1,4–6,26] though reaction with neutral O₂, followed by a second reduction step would also lead to the same intermediates. Regardless, the important point for this discussion is the initial step, that is, the initial electron transfer, and its contrast to the hydroxyl-mediated chemistry.

At the concentrations of the degradation experiments (2 mM substrate, 0.5 g TiO₂ l⁻¹), all substrates have clearly saturated whatever specific binding is available to them and are well into the region of non-specific or multilayer binding. This suggests that the chemoselectivity observed here is related specifically to the structures and/or their particular interactions with the activated TiO₂. It might be argued that the presence of the methyl groups favors demethylation simply because that reaction is unavailable in the other cases. However, the kinetics do not bear that out. From Table 3, it is evident that there is not an obvious connection between more rapid degradation and the presence of alkoxy versus hydroxy substituents. While we have shown that demethylation may occur either by attack of hydroxyl radicals at the methyl group or at the *ipso* aromatic carbon [18], we and others have proposed that the ring-opening reaction is initiated by electron transfer from the aromatic compound to the TiO₂. The different nature of the starting point of these reactions accounts for the different behavior observed here, both as a function of starting material and as a function of addition of isopropyl alcohol as a HO• scavenger.

A hypothesis that accounts for the favoring of the ring-opening reactions where there are hydroxyl groups instead of alkoxy groups is that the hydroxyl groups lead to better “specific” binding to the TiO₂ surface, thus, facilitating the electron transfer process. By “specific”, we mean binding in which presumably deprotonated phenolic groups are directly attached to the TiO₂ surface [7,8]. A similar conclusion that the balance between hydroxyl and electron transfer-based chemistry and hydroxyl chemistry rests with the quality of binding was put forward by Kesselman and co-workers based on kinetic measurements of a Nb-doped TiO₂ electrode for 4-chlorophenol and 4-chlorocatechol [28]. Analogous to that of Martin [8], the data in Fig. 2 show a range of high affinity binding at low concentration, followed by a range of lower affinity adsorption. The latter could be due to multilayer adsorption or simply adsorption at lower affinity (and apparently less chemically active) sites.

Isopropyl alcohol is expected to be a weak competitor for TiO₂ binding sites [29]. The effect of isopropyl alcohol on the binding isotherms for **16** is nearly negligible, slightly dropping the non-specific binding affinity. Nonetheless, a fairly dramatic binding affinity lowering is observed on the isotherm of the more weakly binding **18**, even in the high affinity region. Binding isotherms were not measured for

1,2,4-benzenetriol and **1–4**, but it is reasonable to expect a similar pattern.

The effect of the *i*-PrOH on the product distributions and kinetics is telling. It has been interpreted as acting mainly as a hydroxyl radical scavenger in similar applications [30–37], but this may be a simplification of the overall situation [29,38]. Nonetheless, it is the compounds that originally show mainly HO_{ads}[•]-based chemistry whose degradation rate constants are dropped most significantly (Table 3), and the parallelism between this and the relative loss of hydroxylated/demethylated products at approximately constant conversion is clear.

The kinetics of degradation also merit discussion. Although it is generally the case that the form of Eq. (1) is followed, in which a zero-order dependence of the initial rate on C_0 is found at high C_0 (i.e. $KC_0 \gg 1$), Cunningham observed a zero-order dependence on the rate of 4-chlorophenol degradation down to nearly zero concentration at high photon flux [29]. By contrast, Emeline observed nearly the same phenomenon at low photon flux with phenol [21]. Stafford reported a zero-order dependence on the rate of decay of 4-chlorophenol as long as all the light was absorbed [39]. In these experiments, only the compound is different, not any of the other parameters. Except to note that the two compounds that show the zero-order effect are presumably among the weakest binders in the group, we cannot reasonably speculate on the origin of this phenomenon without further data.

It is now well understood that mere conformation to the form of Eq. (1) does not imply that the straightforward LH mechanism in which the organic is pre-adsorbed to the TiO₂ prior to light absorption and activation [19,21,29,40]. While it has been shown that there is a correlation between the sorbed concentration of 4-chlorocatechol and the macroscopic rate of degradation in a closely related system [7], it is also known that the constant K from Eq. (1) may correspond to more complex equilibria and in any event does not correspond well with dark binding constants [41]. Turchi and Ollis showed that this general form could be followed regardless of whether the oxidant or the organic was adsorbed [19]. Very recent studies have centered on determining whether pre-association is necessary (LH model) or whether the organic may diffuse onto the activated TiO₂ to react (ER model) [21,42]. We suggest that the answer to this may depend on the type of chemistry being observed.

If it is hypothesized that surface bound hydroxyl radicals are considerably longer lived than are valence band holes — not the least because the latter are precursors to the former — then it may be the case that pre-adsorption (i.e. the LH case) is required for the electron transfer-type chemistry, while either LH or ER could be realized for hydroxyl-type chemistry. As a result, two different reactions of the same compound might show different responses to light intensity, catalyst loading, and/or electron accepting additives [21,29]. Emeline predicts very different behaviors with light intensity for k_{LH} and K with respect to light intensity for LH and ER

models. It may thus be quite important to understand the fundamental nature of the chemistry when interpreting such data.

5. Conclusions

Capping the exposed hydroxy groups of multiply hydroxylated benzenes causes a dramatic change in the product distribution in the early degradation steps. Hydroxylation and demethoxylation become predominant over ring-opening chemistry. It is hypothesized that this is because the former two reactions are hydroxyl radical-based chemistry, while the ring-openings are initiated by electron transfer, and further that the electron transfer reactions require tight binding to the photocatalyst at the moment of excitation. The implication of this is that for some degradations, both LH and ER mechanisms might both be active when both electron transfer and hydroxyl radical chemistry may be important.

Acknowledgements

The support of this work by the NSF in the form of a CAREER award is gratefully acknowledged.

References

- [1] X. Li, J.W. Cabbage, T.A. Tetzlaff, W.S. Jenks, *Org. Chem.* 64 (1999) 8509–8524.
- [2] X. Li, J.W. Cabbage, W.S. Jenks, *Org. Chem.* 64 (1999) 8525–8536.
- [3] L. Amalric, C. Guillard, N. Serpone, P. Pichat, *Environ. Sci. Health A A28* (1993) 1393–1408.
- [4] L. Cermenati, P. Pichat, C. Guillard, A. Albini, *J. Phys. Chem. B* 101 (1997) 2650–2658.
- [5] L. Cermenati, A. Albini, P. Pichat, C. Guillard, *Res. Chem. Intermed.* 26 (2000) 221–234.
- [6] F. Soana, M. Sturini, L. Cermenati, A. Albini, *J. Chem. Soc., Perkin Trans. 2* (2000) 699–704.
- [7] J.M. Kesselman, N.S. Lewis, M.R. Hoffmann, *Environ. Sci. Technol.* 31 (1997) 2298–2302.
- [8] S.T. Martin, J.M. Kesselman, D.S. Park, N.S. Lewis, M.R. Hoffmann, *Environ. Sci. Technol.* 30 (1996) 2535–2545.
- [9] DeGussa, DeGussa Tech. Bull. 56 (1984) 8.
- [10] A. Negro, M.J. Garzón, J.F. Martin, A. El Marini, M.L. Roumestant, R. Lázaro, *Synth. Commun.* 21 (1991) 359–369.
- [11] N.S. Sydney, S. Herman, *J. Org. Chem.* 23 (1958) 1559–1560.
- [12] R.K. Ralph, G. Shaw, R.N. Naylor, *J. Chem. Soc.* (1959) 1169–1178.
- [13] M.M. Kayser, L. Breaux, S. Eliev, P. Morand, H.S. Ip, *Can. J. Chem.* 64 (1986) 104–109.
- [14] D. Kyriacou, T.P. Tougas, *J. Org. Chem.* 52 (1987) 2318–2319.
- [15] R.E. Gall, L. Tarasoff, *Aust. J. Chem.* 28 (1975) 687–691.
- [16] R. Willstatter, H.E. Müller, *Chem. Ber.* 44 (1911) 2182–2191.
- [17] J. Knuutinen, I.V.V. Korhonen, *Org. Mass. Spectrom.* 22 (1987) 70–74.
- [18] X. Li, W.S. Jenks, *J. Am. Chem. Soc.* 122 (2000) 11864–11870.
- [19] C.S. Turchi, D.F. Ollis, *J. Catal.* 122 (1990) 178–192.
- [20] A.V. Emeline, A.V. Rudakova, V.K. Ryabchuk, N. Serpone, *J. Phys. Chem. B* 102 (1998) 10906–10916.
- [21] A.V. Emeline, V. Ryabchuk, N. Serpone, *J. Photochem. Photobiol. A* 133 (2000) 89–97.

- [22] M.A. Fox, C.C. Chen, *J. Am. Chem. Soc.* 103 (1981) 6757–6759.
- [23] M.A. Fox, B.L. Lindig, C.-C. Chen, *J. Am. Chem. Soc.* 104 (1982) 5828–5829.
- [24] M.A. Fox, C.-C. Chen, *Tetrahedron Lett.* 24 (1983) 547–550.
- [25] M.A. Fox, in: N. Serpone, E. Pellizzetti (Eds.), *Mechanistic Photocatalysis in Organic Synthesis*, Wiley, New York, 1989, pp. 421–455.
- [26] L. Amalric, C. Guillard, P. Pichat, *Res. Chem. Int.* 20 (1994) 579–594.
- [27] Y. Moro-oka, C.S. Foote, *J. Am. Chem. Soc.* 98 (1976) 1510–1514.
- [28] J.M. Kesselman, O. Weres, N.S. Lewis, M.R. Hoffmann, *J. Phys. Chem. B* 101 (1997) 2637–2643.
- [29] J. Cunningham, P. Sedlak, *J. Photochem. Photobiol. A* 77 (1994) 255–263.
- [30] C. Richard, A.M. Martre, P. Boule, *J. Photochem. Photobiol. A* 66 (1992) 225–234.
- [31] C. Richard, *J. Photochem. Photobiol. A* 72 (1993) 179–182.
- [32] C. Richard, *New J. Chem.* 18 (1994) 443–445.
- [33] C. Richard, P. Boule, *J. Photochem. Photobiol. A* 84 (1994) 151–152.
- [34] C. Richard, P. Boule, *New J. Chem.* 18 (1994) 547–552.
- [35] C. Richard, P. Boule, *Sol. Energy Mater. Sol. Cells* 38 (1995) 431–440.
- [36] T. Shehili, P. Boule, J. LeMaire, *J. Photochem. Photobiol. A* 50 (1989) 103–116.
- [37] T. Shehili, P. Boule, J. LeMaire, *J. Photochem. Photobiol. A* 50 (1989) 117–127.
- [38] J.M. Warman, M.P. De Haas, P. Pichat, N. Serpone, *J. Phys. Chem.* 95 (1991) 8858–8861.
- [39] U. Stafford, K.A. Gray, P.V. Kamat, *J. Catal.* 167 (1997) 25–32.
- [40] H. Kawaguchi, *Environ. Technol.* 15 (1994) 183–188.
- [41] J. Cunningham, G. Al-Sayyed, *J. Chem. Soc. Faraday Trans.* 86 (1990) 3935–3941.
- [42] R. Andreozzi, V. Caprio, A. Insola, G. Longo, V. Tufano, *J. Chem. Technol. Biotechnol.* 75 (2000) 131–136.